Aquatic Botany
June 2022, Volume 179, Pages 103515 (9p.)
https://doi.org/10.1016/j.aquabot.2022.103515
https://archimer.ifremer.fr/doc/00755/86661/

Seasonal changes in the photophysiology of *Ulva batuffolosa* in a coastal barrier reef

Jauffrais Thierry [1, *], Brisset Maele [1], Lagourgue Laura [2], Payri Claude E. [2], Gobin Siloë [2], Le Gendre Romain [1], Van Wynsberge Simon [1]

[1] Ifremer, IRD, Univ Nouvelle-Calédonie, Univ La Réunion, CNRS, UMR 9220 ENTROPIE, BP 32078, 98800, Nouméa, New Caledonia
[2] IRD, Ifremer, Univ Nouvelle-Calédonie, Univ La Réunion, CNRS, UMR 9220 ENTROPIE, BP A5, 98848 Nouméa cedex, New Caledonia

* Corresponding author : Thierry Jauffrais, email address : thierry.jauffrais@ifremer.fr

Abstract :

To assess the photophysiological capacity of the recently described Ulva batuffolosa to form blooms in coral reefs, we monitored its biomass and photophysiological capacity with pulse amplitude modulated (PAM) fluorometry over a year period on a coastal barrier reef in New Caledonia, along with temperature and light. Effective and maximum quantum efficiencies of the photosystem II measured on this Ulva species indicated that the algae was in a “good health” all over the year with high quantum efficiencies under either light (Fq’/Fm’) or dark incubated conditions and (Fv/Fm). Photo-acclimation and -regulation status used by this Ulva sp. were driven by seasons (i.e., light and temperature) in the lagoon. Although photo-inhibition was an evidence during the warm period, U. batuffolosa was overall well adapted to tolerate the range of irradiance and temperature that characterized the lagoon over the year, which suggests that photosynthesis is not an impediment to green tides by this species.

Highlights

► Photo-acclimation and regulation status of *Ulva batuffolosa* were modulated by season. ► *Ulva batuffolosa* was well adapted to support and tolerate high irradiance. ► The combination of elevated temperatures and light damaged its physiology.

Keywords : bloom, coral reef, chlorophyte, pulse amplitude modulated fluorometer, Ulva batuffolosa, rapid light curve, NPQ

1. Introduction

The photophysiological capacity of *Ulva* species is a key factor that determine their ability to form massive blooms (Cui et al., 2015; Wang et al., 2016; Huo et al., 2021), but it has mainly been characterized in temperate areas and subtropical estuaries, e.g., the Yellow sea, the southern coast of Brazil and Florida (Scherner et al., 2012; Xu et al., 2014; Whitehouse and Lapointe, 2015; Zhang et al., 2015, Huo et al., 2021). By contrast, the photophysiological response of *Ulva* species to face environmental stresses is not clearly defined in tropical and subtropical shallow coral reef lagoons. In these lagoons, temperature is higher than in temperate ecosystems, and light can be higher over longer period. These habitats are characterized by clear waters with a high penetration depth of the photosynthetically active radiation (PAR), up to 2000 µmol m^{-2} s^{-1} (Kirk, 1994; Pringault et al., 2005), and ultraviolet radiation, up to 2 W m^{-2} for UVB and 40 W m^{-2} for UVA (Torregiani and Lesser, 2007; Conan et al., 2008; Courtial et al., 2017). In fact, light intensity may fluctuate significantly from second to seasonal scale, with fluctuations that are predictable (e.g., day length and light angle, tide) and others that are not (e.g., cloudiness, lagoon turbidity caused by terrestrial run-off or sediment resuspension). In these habitats, *Ulva* must cope with fluctuating light to optimize its use for photosynthesis and to protect their photosystems from excessive light (Henley and Ramus, 1989; Carr and Björk, 2007, Goss and Jakob, 2010; Zhang et al., 2015). Previous studies on temperate species highlighted the great ability and plasticity of *Ulva* to cope with light (Carr and Björk, 2007, Zhang et al., 2015). *Ulva* species (e.g., *U. prolifera* and *U. lactuca*) were able to keep high photosynthetic capability using the plasticity of the surface and lower layers of their thalli, modifying their pigment content and using NPQ, D1 protein, energy redistribution between PSII/PSI and fast recovery ability under low light to avoid irreversible damage to their PSII and PSI (Carr and Björk, 2007; Zhang et al., 2015; Wang et al., 2016).

Algae exposed to excessive light energy can implement three processes: photo-adaptation, acclimation and regulation (Falkowski and Laroche, 1991; Raven and Geider, 2003; Huot and Babin, 2010). Photo-adaptation is a long term and genetic process, while photo-acclimation is explained by the

macromolecular modification of a species from hours to days/seasonal light conditions (Falkowski and Laroche, 1991; Raven and Geider, 2003; Huot and Babin, 2010). At this time scale, the genetic make-up does not change but the algae can modify the number and size of its photosynthetic apparatus and associated pigments. Finally, photo-regulation processes are more dedicated to manage rapid changes in the light regimes (seconds to minutes) to quickly protect (lower or prevent damages) photosystems from excessive light energy, but without *de novo* synthesis or break down of molecules (Falkowski and Laroche, 1991; Raven and Geider, 2003; Huot and Babin, 2010). It can be achieved by quenching the photochemistry through non-photochemical processes, which dissipates the excitations in the antennae complex into heat (Consalvey et al., 2005).

Photosynthesis irradiance curves have been used in the past to assess the effect of environmental factors on macroalgae physiology (Lapointe, 1981), including *Ulva* species (Figueroa et al., 2009; Scherner et al., 2012; Xu et al., 2014; Whitehouse and Lapointe, 2015; Wang et al., 2016). In this scenario, pulse amplitude modulated (PAM) fluorometry is a powerful and commonly used technique based on chlorophyll *a* fluorescence (Krause and Weis, 1991; Schreiber et al., 1994; Maxwell and Johnson, 2000). It offers the advantage to be fast (Schreiber et al., 1994) and is often used to assess photophysiological response of micro and macroalgae under stressful conditions (Figueroa et al., 1997; Figueroa et al., 2009; Scherner et al., 2012; Whitehouse and Lapointe, 2015; Coulombier et al., 2021). Although it has proven to be a useful and powerful tool for the studies of macroalgae photophysiology (Ralph and Gademann, 2005), this approach is often considered biased for macroalgae. Variations in the fluorescence signal due to the thickness of macroalgae tissues often hampers direct comparison with oxygenic photosynthesis measurements particularly at high irradiance and comparison between species (reviewed in Enriquez and Borovitzka, 2010). Although imperfect, the use of relative electron transport rate (rETR) values instead of ETR is recommended to reduce problems associated with absorptance (*i.e.*, the fraction of incident light absorbed by pigmented tissue) particularly if the organisms or tissues examined have similar absorption cross-sections (Beer et al. 2001; Ralph et al., 2002; Enriquez and Borovitzka, 2010). PAM fluorometry also allows to characterize photophysiological state, through the study of dark and light incubated algae. Light incubated algae have their photosynthetic apparatus adapted to manage the ambient light, *i.e.*, all

photo-regulation processes are active; whereas, dark incubated algae have downregulated all photosynthetic mechanisms that usually help the algae to cope with the ambient light but without modifying their acclimated macromolecular compounds (Huot and Babin, 2010).

In this study, we monitored the photophysiological capacity of *Ulva batuffolosa*, a species involved in green tides, in a shallow tropical lagoon in New Caledonia, over a year period. We collected the *Ulva sp.* at different seasons and used PAM fluorometry to quantify their PSII quantum efficiency, maximum relative electron transport rate, their capacity to cope with light at low and high irradiance under light or dark incubated conditions, and to dissipate the excess of energy via Non-Photochemical Quenching (NPQ). All measurements were acquired to provide an overview of the physiological state of *Ulva batuffolosa* owing to environmental and seasonal (light and temperature) photo-acclimation and photo-regulation status.

2. Materials and method

2.1. Study area

New Caledonia is located in the Southwestern Pacific Ocean, ~1 500 km east of Australia (Fig. 1). It comprises one main large island, known as Grande Terre, bordered by a 1 600 km long barrier reef, which delimits a 23 400 km² lagoon (Andréfouët et al., 2009). The present study focuses on the Poé-Gouaro-Déva (PGD) lagoon (21.62°S, 165.38°E) located on the west coast of Grande Terre (Fig. 1), a hotspot of tourism activities and one of the Caledonian lagoons registered at the UNESCO World Heritage sites. In this study, we focus on green algal mats located around B21 station in the northwestern part of the PGD lagoon (Fig. 1), at the limit between a wide seagrass bed that borders the coastline and sandy soft-bottom habitats. Blooms of *U. batuffolosa* in this area were the main cause of the two green tides that occurred in January 2018 and June 2019 (Brisset et al., 2021; Lagourgue et al., *in press*). In this shallow area (maximum depth ~2 m), the seagrass bed is not homogeneous and can be intertwined with patches of coral communities (branching *Montipora* and *Acropora*) and sand.

2.2. Field sampling

Five field campaigns were performed at 2-4 months intervals to collect green algae and estimate their cover, the 16th May 2019, 09th July 2019, 18th November 2019, 19th February 2020, and 25th May 2020, respectively. The cover of green macroalgae was estimated along three line intersect transects of 10 m length. Transects were not permanently established, but their location was geo-referenced (handheld GPS Garmin) with a 10–20 m uncertainty, and they were always performed at similar depth and on the same habitat. Along each transect, two to three 0.25 m² quadrats were placed on algal patches. All green algae inside quadrats were collected and stored in plastic bags in a cooler for further analyses. For the three last field campaigns, as *Ulva* were rare and absent on transects (see results), samples were collected within a larger screening area (~ 10 000 m²) around transects.

2.3 Temperature and light condition before and during sampling

Light and temperature that affected the area all along the study period were acquired using regional models and *in situ* instruments.

Light above the water surface was measured during each field campaign using a light meter (Li-cor) and a Li-192 quantum sensor (Li-cor). Light conditions that characterized the PGD area before and during sampling were also extracted from the ERA5 atmospheric reanalysis (Hersbach et al., 2020). This model provides an hourly time series of variables such as the Surface Solar Radiation Downwards (SSRD, KJ m^{-2}) with a one hour time step at 0.25° long and 0.25° lat spatial resolution. For this study, we used data extracted from the nearest grid point to the PGD lagoon (21.75°S 165.25°E).

Lagoon temperature was recorded from February 2019 to May 2020 at station B21, or near to it, with high accuracy (±0.002 °C) using RBR® duo loggers. Since gaps affected the time series during one inter-season (no data recorded between 16th May and 09th July 2019), the time series was filled with satellite derived sea surface temperature (SST) estimates. Sea surface temperature was extracted from the Global, daily Multi-scale Ultra-high Resolution (MUR) SST analysis at 0.01° (around 1 km) resolution (Chin et al., 2017; https://mur.jpl.nasa.gov/). Data were also retrieved from the nearest grid point from field transects. Comparison with *in situ* temperature data recorded by the logger and SST estimates highlighted a median difference of ± 0.7 °C. The maximum daily difference reached 2.7 °C

during the warm period, but SST data were deemed suitable for the purpose of this study since lower bias were found during inter-seasons (Supplement material SM1).

2.4. Algae biomass estimation

The biomass of green algae collected inside each quadrat was determined, all genera confounded. Algae were weighted after sampling (wet weight), and after a drying period at 50°C until a constant weight value was obtained. The resulting biomass (dry weight) was averaged among quadrats (B_Q, g m^{-2}) and pondered by the percentage of cover of green algae along the transect (C_T, %) to infer biomass at transect scale (B_T, g m^{-2}, equation 1).

$$B_T = B_Q \times C_T \quad \text{(eq. 1)}$$

2.5. Algae identification

The specimens sampled along each transect were sorted under binocular, pressed-dried on herbarium sheets and housed at NOU (herbarium abbreviation follows Thiers (2019)). Fragments were subsampled and preserved in a formaldehyde solution (5% in seawater added with borax) for further taxonomical analysis and ethanol 95% for DNA analyses. Morphological and histological observations were performed using an Axio Imager A2 microscope (ZEISS, Oberkochen, Germany) fitted with a Canon EOS 100D camera (Canon, Tokyo, Japan). Species identification were based on the most relevant literature references for *Ulva* species, including Kraft et al. (2010), Horimoto et al. (2011), Masakiyo et al. (2014), Krupnik et al. (2018), Melton et al. (2020) and Xie et al. (2020). DNA analyses were conducted separately and are part of a comprehensive phylogenetic and molecular taxonomy study of the Ulvales from New Caledonia (Lagourgue et al. *in press*).

2.6. Photosynthetic parameters of Ulva batuffolosa *over a one-year-period*

Pulse Amplitude Modulated (PAM) fluorometry measurements were performed during each field campaigns, to provide an overview of the physiological state of the bloom forming *U. batuffolosa* in a

diversity of environmental conditions. All measurements were performed under light or dark incubated conditions to discriminate photo-acclimation and photo-regulation status.

Photosynthetic parameters were measured with a PAM chlorophyll fluorometer (AquaPen-P AP 110-P of Photon Systems Instruments, Czech Republic) with a blue light at 470 nm. All measurements were carried in a Petri dish (10 cm × 1.5 cm) filled with filtered sea water (50-75 mL, 0.2 µm) on the apical region of *U. batuffolosa* to avoid a potential impact of self-shaded region. Following microscopic identification, fragments of apical regions were cut and maintained with a perpendicular orientation under the submersible optical probe of the PAM fluorometer. The set up was then placed in a black box to avoid disturbance of ambient light during measurements. All measurements were done in triplicate, each time on new fragments to avoid trouble due to light exposure from previous measurements.

Light incubated measurements were carried out immediately after sampling on the boat (Aldric, 5.6 m Stabicraft), while, dark measurements were carried out following a dark (very low light 1-2 µmol photons m^{-2} s^{-1}) adaptation of one hour in the laboratory. In between, the samples were kept in relative darkness (2 µmol photons m^{-2} s^{-1}) in a cooler during transport to the laboratory, with a small amount of *Ulva* in a large quantity of seawater (2 L) from the sampling site.

The effective and maximum PSII quantum efficiency (Fq'/Fm' and Fv/Fm) were measured under light and dark incubated conditions, respectively. These measures were acquired with a saturating pulse at 3000 µmol photons m^{-2} s^{-1} (Table 1; Schreiber et al., 1994; Consalvey et al., 2005).

Rapid light curves were performed under light and dark incubated conditions with seven incremental irradiances steps (10; 20; 50; 100; 300; 500 and 1 000 µmol photons m^{-2} s^{-1}) of 60 s. The *Ulva* photophysiological parameters ($rETR_{max}$ (AU), alpha (α), beta (β) and Ek) were estimated by adjusting the model by Platt et al. (1980) to the experimental data (Table 1). In addition, the photo regulation capacity via Non-Photochemical Quenching (NPQ) was measured to assess the photo-regulation capacity and recovery of the *Ulva* sp. reaction centers to a continuous illumination of 1 000 µmol photons m^{-2} s^{-1} with 10 successive light pulses at saturating light and followed by darkness for recovery with two quantum efficiency measurements (only on dark incubated *Ulva*). These NPQ measurements; however, could not be performed during the first field campaign because of a technical problem (Table 1).

2.7. Statistical analyses

To test statistically the differences in environmental history conditions that affected green algae collected between field campaigns, we used the conditions of light (SSRD) and temperature that occurred along the week before sampling each campaign. Statistical differences between campaigns were tested using ANOVA or Kruskal–Wallis tests when the homoscedasticity and normality hypotheses were not satisfied. When necessary, Fisher's least significant difference (LSD) tests were performed after ANOVA and Dunn's tests were performed after Kruskal-Wallis tests to assess the significance of differences between each pair of sampling campaigns. Correlation between photo-physiological parameters ($rETR_{max}$, alpha, beta, Ek) and environmental parameters (temperature, SSRD, PAR) were tested using the Spearman's non-parametric correlation test. For NPQ, a generalized linear model was used to assess differences between sampling campaigns, and time points generated by repeated NPQ measurements during the NPQ induction by actinic light and dark recovery period. The statistical analyses were carried out using the R studio v1.2.1578 software (©2009–2019 R studio v1.2.1578) for the environmental data and Statgraphics Centurion XV.I (StatPoint Technologies) for the photophysiological data. All results (*i.e.*, PAM measurements and environmental characterization) are expressed as mean ± standard error (SE) in this manuscript.

3. Results

3.1. Temperature and light conditions experienced by collected algae

Over the study period, seawater temperature ranged from 21.46 °C in August 2019 to 29.59 °C in March 2020, with significant short-term variation (Fig. 2). This include a decrease of 2.83 °C in 5 days the week before sampling in July 2019, and an increase of 3.75 °C in 13 days at the end of November 2019. As a result, the *Ulva* species collected during the field campaigns were exposed to different history of temperatures (KW Chi-squared = 29.54; $p < 0.001$), with significantly higher temperature measured in February 2020 (28.09 ± 0.89 °C) before sampling than before all other campaigns (Dunn's test Z ranging between -4.30 and 4.64; $p < 0.05$), except for the May 2019 campaign ($Z = 1.82$; $p = 0.06$; Supplement material SM2). In July 2019 and May 2020, the algae were exposed to

periods of lower temperatures, *i.e.*, 23.27 ± 1.31 °C and 24.13 ± 0.44 °C, respectively. The temperature history experienced by algae sampled in May 2019 and November 2020 were similar (25.53 ± 0.25 °C and 25.40 ± 0.77 °C, p = 0.86, Fig. 2).

Surface Solar Radiation Downwards (SSRD) also followed a seasonal pattern, but reached highest values in late November 2019 (longest days) and lower values in early June (shortest days, Fig. 2). As a result, the *Ulva* collected during the different field campaigns were exposed to different light history (KW Chi-squared = 23.52; $p < 0.001$), with higher values in November 2019 (2 111 ± 1 345 KJ m^{-2}) than during the other sampling periods (Dunn's test Z ranging from -3.28 to 4.40, $p < 0.01$). The lowest SSRD were measured the weeks before July 2019 (893 ± 787 KJ m^{-2}), May 2019 (991 ± 868 KJ m^{-2}), and May 2020 (1 065 ± 884 KJ m^{-2}) field campaigns. Photosynthetic Active Radiation (PAR) measured during field campaigns were higher in November 2019 (2042 ± 51 µmol photons m^{-2} s^{-1}), than during other field campaigns (May 2019, 1746 ± 41 µmol photons m^{-2} s^{-1}; July 2019, 1838 ± 43 µmol photons m^{-2} s^{-1}; February 2020, 1921 ± 42 µmol photons m^{-2} s^{-1}). The lowest values of PAR were found in May 2020, 344 ± 36 µmol photons m^{-2} s^{-1}), because of a cloudy weather during this last field campaign.

3.2. Biomass of green algae

Green algae were abundant during the first two field campaigns, with higher biomass in July 2019 (B_T = 69.83 ± 17.10 gDW m^{-2}) than in May 2019 (B_T = 8.80 ± 1.59 gDW m^{-2}). During the three other field campaigns, green algae were rare, with no biomass along the three transects nor inside quadrats (Fig. 3). However, *Ulva batuffolosa* was still present around transects.

3.3. Algae identification

Among the macroalgae identified along or nearby transects in this study, *Ulva batuffolosa* was largely predominant. This species forms dense and moving tufts of entangled, tubular, and branched filaments. Main axes are variable in size but usually measure ~100 µm or more in diameter, while secondary branches are smaller. They are composed of rectangular to polygonal cells (20*25*20 µm) with regular contours, forming a coherent mat (Lagourgue et al. *in press*; Supplement Material SM3)

of several decimeters in length. They can attach to corals and seagrass, or drift in the water with the currents. This species corresponds to *Ulva* sp.3 in Brisset et al. (2021).

3.4. Photosynthetic parameters of the Ulva *sp.*

The effective (Fq'/Fm') and maximum quantum (Fv/Fm) light utilization efficiency of the *Ulva* sp., *i.e*., a proxy of the efficiency of the PSII in using light for photochemical conversion, measured under light and dark incubated condition showed high values with Fq'/Fm' = 0.45 ± 0.6 and Fv/Fm = 0.66 ± 0.05, but did not show very high differences between the five studied periods. No significant differences between campaigns were found for Fq'/Fm' ($p = 0.10$) and solely the Fv/Fm measured during the last sampling period in May 2020 was significantly lower ($p = 0.042$, Fv/Fm = 0.58 ± 0.03) than the other ones (Fv/Fm > 0.66, Fig 4B, Table 2).

Differences between sampling campaigns were clearly visible using the data extracted from the RLCs (Table 2, Fig 5 and 6). The maximum electron transport rate ($rETR_{max}$) measured under light or dark incubated conditions were both significantly different with P values below 0.01 (Table 2). This proxy of the photosynthetic activity increased from May 2019 (70 ± 5 AU light incubated condition, 119 ± 2 AU dark incubated condition) to July 2019 (105 ± 4 AU light incubated condition and 131 ± 2 AU dark incubated condition) and then decreased. Light incubated $rETR_{max}$ values were not statistically different from November 2019 until the end of the survey (Fig. 6A, yellow bars); whereas the decrease was more gradual regarding dark incubated values (Fig. 6A, grey bars).

Similarly, the light saturation coefficient (Ek), used here as a proxy of *U. batuffolosa* ability to use "high light" intensity, was also significantly higher in July 2019 than for other sampling campaigns, either for light incubated measurements (534 ± 43 µmol photons m^{-2} s^{-1} versus between 140 and 240 µmol photons m^{-2} s^{-1}, $p < 0.001$) and for dark incubated measurements (526 ± 23 µmol photons m^{-2} s^{-1} *versus* between 300 and 380 µmol photons m^{-2} s^{-1}, $p < 0.05$, Fig 6B and Table 2).

The maximum light utilization coefficients, alpha (α), used as a proxy of the algal ability to use "low light" intensity, were also significantly different between periods (Fig 6C and Table 2), but these differences were weaker compared to $rETR_{max}$ and E_k (Table 2). The lowest alpha values were observed in July 2019 (0.21 ± 0.01 light incubated condition and 0.25 ± 0.02 dark incubated condition)

and the highest one in May 2019 (0.31 ± 0.04 light incubated condition and 0.32 ± 0.01 dark incubated condition).

The photoinhibition coefficient, beta (β) (Fig 6D; Table 2), was significantly different from zero for RLCs carried out under light incubated condition in February and May 2020 only (Fig 5A), and was higher in February than in May 2020 ($p < 0.05$, Table 2).

The NPQ measurements induced by the actinic light (yellow background on Fig. 7) and dark recovery (grey background) period were implemented to assess the photo-regulation capacity (*i.e.*, the capacity to dissipate the excess of energy as heat) and recovery via NPQ during and following an exposure to light. During the four field campaigns for which NPQ measurements were performed (Fig. 7), July 2019 to May 2020, NPQ was used by the *Ulva* sp. to protect their PS against an excess of light energy. However, the magnitude of NPQ induction and recovery was significantly greater in February 2020 and lower in November 2019 (Fig. 7; Table 3). In addition, no NPQ recovery was observed in May 2020. No significant correlation between photo-physiological parameters and environmental data could be evidenced with the Spearman non-parametric correlation tests, but the correlation between beta (light incubated) and temperature was near the significant level (rho = 0,87; p = 0,054; Supplement Material SM4).

4. Discussion

The photosynthetic seasonal acclimation of *U. batuffolosa* was observable by comparing field campaigns using both light and dark incubated data. *U. batuffolosa* increased its light-harvesting capacity (high $rETR_{max}$) under "low-light" austral autumn/winter conditions (*i.e.*, May and July 2019, Fig. 5 and 6A). On the contrary, *U. batuffolosa* lowered its $rETR_{max}$ under "high-light" austral summer conditions (*i.e.*, November 2019 and February 2020, Fig. 5). Such acclimation can either be achieved by increasing the number or the size of photosynthetic units (Richardson et al., 1983; Falkowski and Laroche, 1991; Beer et al., 2014). When the number of photosynthetic units (PSU) increases (under low light condition) then both the antenna size and the number of reaction centers increase, enhancing the functionality of the photosynthetic apparatus (*i.e.*, higher rETRmax, alpha and Ek, Beer et al., 2014). Whereas, if only the size of photosynthetic units increases under low-light conditions, this should decrease the maximal photosynthetic productivity while increasing the light utilization

efficiency (alpha) (Richardson et al., 1983; Beer et al., 2014). In the present study, *U. batuffolosa* $rETR_{max}$ and E_k were higher for the *Ulva* collected during field campaigns characterized by lower irradiance (PAR) and SSRD history, while the response of alpha is unclear, indicating that photo-acclimation was achieved through the adjustment of the number of PSU to maximize light utilization during the lower light austral winter period rather than through the size of the PSU. However, algae collected in May 2020 escaped the trend, suggesting that acclimation capacity of algae was also dependent on other environmental factors (e.g., nutrient availability). N-limitation may gradually cause a decrease in photosynthetic pigments (Geider et al., 1993), a decline in Fv/Fm (Cleveland and Perry, 1987; Berges et al., 1996; Jauffrais et al., 2016) and the gradual inactivation of the protein D1 in PSII reaction centers (Campbell and Tyystjarvi, 2012). Protein D1 is a key component in the electron transport chain and its turnover is often a limiting factor in PSII repair rates (Campbell and Tyystjarvi, 2012).

In February 2020, *U. batuffolosa* was stressed by the environmental conditions, as shown by the presence of photoinhibition (beta > 0). Photoinhibition could be induced by the high light availability and the higher temperature (>28°C). In May 2020, although Fv/Fm was still relatively high, other photophysiological data indicated that *U. batuffolosa* was living under stressful conditions at the end of the study (rETRmax and β), which was supported by the decline and almost absence of *U. batuffolosa* biomass in the lagoon (Fig. 3). This decrease in photosynthetic capacity of *U. batuffolosa* over the study period probably result from the combined effect of season (light and temperature) and a suggested N-limitation, which could explain the decrease in $rETR_{max}$, finally leading to the induction of photoinhibition in February and May 2020.

Non-photochemical quenching (NPQ) is a common and important mechanism utilized by algae to tolerate and prevent damages to photosystems, owing to sudden high or fluctuating light levels, by heat dissipation of excessive light energy (Franklin et al., 1992;Uhrmacher et al., 1995; Schofield et al., 1998; Bischof et al., 2006; Enríquez and Borowitzka, 2010). *U. batuffolosa* utilized NPQ over all surveys, *i.e.*, during both austral summer and winter, owing to the high solar irradiance in New Caledonia all year around. NPQ is thus an important photo-regulation mechanism utilized by *U. batuffolosa* in the PGD lagoon, which allows to prevent or minimize photoinhibition in response to

short-term changes in irradiance and to maximize photosynthesis and productivity under the high irradiance of this shallow coral reef habitat.

However, NPQ can become exhausted under excessive light especially if amplified by other environmental pressure. Reduced NPQ efficiency and lower recovery capacity, such as the difference observed between February and May 2020, can damage protein D1 leading to a decline in photosynthetic efficiency, chronic photoinhibition and production of ROS (Franklin and Forster, 1997), which may be enhanced by high temperature and nutrient limitation (Franklin, 1994; Campbell et al., 2006). The decline of $rETR_{max}$ until the end of the study is thus probably due to the exhaustion of photo-regulation mechanisms (e.g., NPQ) leading to long-term photoinhibition triggered by the combination of high light and temperature.

5. Conclusion

This study highlights that photo-acclimation and -regulation status of *U. batuffolosa* are mainly driven by seasons (*i.e.*, light and temperature) in New Caledonia. In addition, our data provide significant advances in understanding the ability of this bloom forming species to use and manage light in clear and shallow water habitats. Notably, our study suggests that although *U. batuffolosa* is likely to suffer from long-term and excessive high solar irradiance and high seawater temperatures that will reduce its photosynthetic efficiency and eventually damage its photosynthetic apparatus, this species is still well adapted to support and tolerate the range of irradiance and temperature that characterized shallow tropical lagoon. Thus, it seems that photosynthesis is not an impediment to blooms by this species, which may explain the occurrence of green tides both during the warm and the cold seasons.

Acknowledgments

This project was funded by Direction du développement durable des territoires, Province Sud, New Caledonia, grant number C.458-19, ELADE project. The South Province of New Caledonia delivered the sampling authorizations (N°4406-2018/ARR/DENV).

We would like to thank Miguel Clarke, Benoit Soulard and Alan Choupeau for their logistical support during field campaigns. We also thanks Laurent Millet, Clarisse Majorel, and Claire Bonneville from the “Plateforme du vivant”, where genetic analyses were performed to support algae identification.

CRediT author statement

TJ: conceptualization, methodology, formal analysis, investigation, data curation, writing - reviewing & editing; **MB:** conceptualization, methodology, software, formal analysis, investigation, data curation, writing - reviewing & editing; **LL:** methodology, formal analysis, writing - reviewing & editing; **CP:** conceptualization, writing - reviewing & editing, project administration, funding acquisition; **SG:** formal analysis, investigation; **RL:** methodology, software, formal analysis, investigation, data curation, writing - reviewing & editing; **SVW:** conceptualization, methodology, software, formal analysis, investigation, data curation, writing - reviewing & editing; project administration, funding acquisition

References

Andrefouet, S., Cabioch, G., Flamand, B., Pelletier, B., 2009. A reappraisal of the diversity of geomorphological and genetic processes of New Caledonian coral reefs: a synthesis from optical remote sensing, coring and acoustic multibeam observations. Coral Reefs 28, 691-707.

Beer, S., Björk M., Gademan, R., Ralph, P., 2001. Measurements of photosynthesis in seagrass. In: Short FT, Coles R (eds) Global seagrass research methods. Elsevier, Amsterdam, pp 183–198

Beer, S., Björk, M., Beardall, J., 2014. Photosynthesis in the marine environment. John Wiley & Sons.

Berges, J.A., Charlebois, D.O., Mauzerall, D.C., Falkowski, P.G., 1996. Differential effects of nitrogen limitation on photosynthetic efficiency of photosystems I and II in microalgae. Plant Physiol. 110, 689-696.

Bischof, K., Rautenberger, R., Brey, L., Perez-Llorens, J.L., 2006. Physiological acclimation to gradients of solar irradiance within mats of the filamentous green macroalga *Chaetomorpha linum* from southern Spain. Mar. Ecol. Prog. Ser. 306, 165-175.

Brisset, M., Van Wynsberge, S., Andréfouët, S., Payri, C., Soulard, B., Bourassin, E., Gendre, R.L., Coutures, E., 2021. Hindcast and near real-time monitoring of green macroalgae blooms in shallow coral reef lagoons using sentinel-2: A New-Caledonia case study. Remote Sensing 13, 211.

Campbell, D.A., Tyystjarvi, E., 2012. Parameterization of photosystem II photoinactivation and repair. Biochim. Biophys. Acta 1817, 258-265.

Campbell, S.J., McKenzie, L.J., Kerville, S.P., 2006. Photosynthetic responses of seven tropical seagrasses to elevated seawater temperature. J. Exp. Mar. Biol. Ecol. 330, 455-468.

Carr, H., Bjork, M., 2007. Parallel changes in non-photochemical quenching properties, photosynthesis and D1 levels at sudden, prolonged irradiance exposures in *Ulva fasciata* Delile. J. Photochem. Photobiol. 87, 18-26.

Chin, T.M., Vazquez-Cuervo, J., Armstrong, E.M., 2017. A multi-scale high-resolution analysis of global sea surface temperature. Remote Sens. Environ. 200, 154-169.

Cleveland, J.S., Perry, M.J., 1987. Quantum yield, relative specific absorption and fluorescence in nitrogen limited *Chaetoceros gracilis*. Mar. Biol. 94, 489-497.

Conan, P., Joux, F., Torreton, J.P., Pujo-Pay, M., Douki, T., Rochelle-Newall, E., Mari, X., 2008. Effect of solar ultraviolet radiation on bacterio- and phytoplankton activity in a large coral reef lagoon (southwest New Caledonia). Aquat. Microb. Ecol. 52, 83-98.

Consalvey, M., Perkins, R.G., Paterson, D.M., Underwood, G.J.C., 2005. Pam fluorescence: A beginners guide for benthic diatomists. Diatom Res. 20, 1-22.

Cosgrove, J., Borowitzka, M.A., 2010. Chlorophyll Fluorescence Terminology: An Introduction, in: Suggett, D.J., Prášil, O., Borowitzka, M.A. (Eds.), Chlorophyll a Fluorescence in Aquatic Sciences: Methods and Applications. Springer Netherlands, Dordrecht, pp. 1-17.

Coulombier, N., Blanchier, P., Le Dean, L., Barthelemy, V., Lebouvier, N., Jauffrais, T., 2021. The effects of CO2-induced acidification on *Tetraselmis* biomass production, photophysiology and antioxidant activity: a comparison using batch and continuous culture. J. Biotech. 325, 312-324.

Courtial, L., Roberty, S., Shick, J.M., Houlbrèque, F., Ferrier-Pagès, C., 2017. Interactive effects of ultraviolet radiation and thermal stress on two reef-building corals. Limnol. Oceanogr. 62, 1000-1013.

Cui, J.J., Zhang, J.H., Huo, Y.Z., Zhou, L.J., Wu, Q., Chen, L.P., Yu, K.F., He, P.M., 2015. Adaptability of free-floating green tide algae in the Yellow Sea to variable temperature and light intensity. Mar. Pollut. Bull. 101, 660–666

Enríquez, S., Borowitzka, M.A., 2010. The use of the fluorescence signal in studies of seagrasses and macroalgae, in: Suggett, D.J., Prášil, O., Borowitzka, M.A. (Eds.), Chlorophyll a fluorescence in aquatic sciences: Methods and applications. Springer Netherlands, Dordrecht, pp. 187-208.

Falkowski, P.G., Laroche, J., 1991. Acclimation to spectral irradiance in algae. J. Phycol. 27, 8-14.

Figueroa, F.L., Israel, A., Neori, A., Martinez, B., Malta, E.J., Ang, P., Inken, S., Marquardt, R., Korbee, N., 2009. Effects of nutrient supply on photosynthesis and pigmentation in *Ulva lactuca* (Chlorophyta): responses to short-term stress. Aquat. Biol. 7, 173-183.

Figueroa, F.L., Salles, S., Aguilera, J., Jimenez, C., Mercado, J., Vinegla, B., FloresMoya, A., Altamirano, M., 1997. Effects of solar radiation on photoinhibition and pigmentation in the red alga *Porphyra leucosticta*. Mar. Ecol. Prog. Ser. 151, 81-90.

Franklin, L.A., 1994. The effects of temperature-acclimation on the photoinhibitory responses of *Ulva-rotundata* blid. Planta 192, 324-331.

Franklin, L.A., Forster, R.M., 1997. The changing irradiance environment: consequences for marine macrophyte physiology, productivity and ecology. Eur. J. Phycol. 32, 207-232.

Franklin, L.A., Levavasseur, G., Osmond, C.B., Henley, W.J., Ramus, J., 1992. 2 components of onset and recovery during photoinhibition of *Ulva-rotundata*. Planta 186, 399-408.

Geider, R.J., Laroche, J., Greene, R.M., Olaizola, M., 1993. Response of the photosynthetic apparatus of *Phaeodactylum tricornutum* (Bacillariophyceae) to nitrate, phosphate, or iron starvation. J. Phycol. 29, 755-766.

Goss, R., Jakob, T., 2010. Regulation and function of xanthophyll cycle-dependent photoprotection in algae. Photosynthesis Res. 106, 103-122.

Henley, W.J., Ramus, J., 1989. Time course of physiological-response of *Ulva-rotundata* to growth irradiance transitions. Mar. Ecol. Prog. Ser. 54, 171-177.

Hersbach, H., Bell, B., Berrisford, P., Hirahara, S., Horányi, A., Muñoz-Sabater, J., Nicolas, J., Peubey, C., Radu, R., Schepers, D., Simmons, A., Soci, C., Abdalla, S., Abellan, X., Balsamo, G., Bechtold, P., Biavati, G., Bidlot, J., Bonavita, M., De Chiara, G., Dahlgren, P., Dee, D., Diamantakis, M., Dragani, R., Flemming, J., Forbes, R., Fuentes, M., Geer, A., Haimberger, L., Healy, S., Hogan, R.J., Hólm, E., Janisková, M., Keeley, S., Laloyaux, P., Lopez, P., Lupu, C., Radnoti, G., de Rosnay, P., Rozum, I., Vamborg, F., Villaume, S., Thépaut, J.-N., 2020. The ERA5 global reanalysis. Quarterly Journal of the Royal Meteorological Society 146, 1999-2049.

Horimoto, R., Masakiyo, Y., Ichihara, K., 2011. Enteromorpha-like *Ulva* (Ulvophyceae, Chlorophyta) growing in the Todoroki river, Ishigaki island, Japan, with special reference to *Ulva meridionalis* Horimoto et Shimada, sp. nov.. Bull. Natl. Museum Nat. Sci. Ser. B, Bot. 37, 155–167.

Huot, Y., Babin, M., 2010. Overview of fluorescence protocols: Theory, basic concepts, and practice, in: Suggett, D.J., Prášil, O., Borowitzka, M.A. (Eds.), Chlorophyll a fluorescence in aquatic sciences: Methods and applications. Springer Netherlands, Dordrecht, pp. 31-74.

Huo, Y., Kim, J.K., Yarish, C., Augyte, S., He, P., 2021. Responses of the germination and growth of Ulva prolifera parthenogametes, the causative species of green tides, to gradients of temperature and light. Aquat. Bot. 170, 103343.

Jauffrais, T., Jesus, B., Méléder, V., Turpin, V., Russo, A.D.A.P.G., Raimbault, P., Martin-Jézéquel, V., 2016. Physiological and photophysiological responses of the benthic diatom *Entomoneis paludosa* (Bacillariophyceae) to dissolved inorganic and organic nitrogen in culture. Mar. Biol. 163, 1-14.

Kirk, J.T.O., 1994. Light and Photosynthesis in Aquatic Ecosystems, 2 ed. Cambridge University Press, Cambridge.

Kraft, L.G.K., Kraft, G.T., Waller, R.F., 2010. Investigations into southern Australian *Ulva* (Ulvophyceae, Chlorophyta) taxonomy and molecular phylogeny indicate both cosmopolitanism and endemic cryptic species. J. Phycol. 46, 1257–1277.

Krause, G.H., Weis, E., 1991. Chlorophyll fluorescence and photosynthesis - the basics. Annu. Rev. Plant. Physiol. Plant. Mol. Biol. 42, 313-349.

Krupnik, N., Rinkevich, B., Paz, G., Douek, J., Lewinsohn, E., Israel, A., Carmel, N., Mineur, F., Maggs, C.A., 2018. Native, invasive and cryptogenic *Ulva* species from the Israeli Mediterranean Sea: Risk and potential. Mediterr. Mar. Sci. 19, 132–146.

Lagourgue, L., Gobin, S., Brisset, M., Vanderberghe, S., Bonneville, C., Jauffrais, T., Van Wynsberge, S., Payri, C.E., 2022. Ten new species of *Ulva* (Ulvophyceae, Chlorophyta) discovered in New Caledonia: Genetic and morphological diversity, and bloom potential. Eur. J. Phycol. 1-21. In press. https://doi.org/10.1080/09670262.2022.2027023

Lapointe, B.E., 1981. The effects of light and nitrogen on growth, pigment content, and biochemical-composition of *Gracilaria-foliifera* v *Angustissima* (gigartinales, rhodophyta). J. Phycol. 17, 90-95.

Liu, D.Y., Keesing, J.K., Xing, Q.U., Shi, P., 2009. World's largest macroalgal bloom caused by expansion of seaweed aquaculture in China. Mar. Pollut. Bull. 58, 888-895.

Maxwell, K., Johnson, G.N., 2000. Chlorophyll fluorescence - a practical guide. J. Exp. Bot. 51, 659-668.

Masakiyo, Y., Shimada, S., 2014. Species Diversity of the genus Ulva (Ulvophyceae, Chlorophyta) in Japanese waters, with special reference to *Ulva tepida* Masakiyo et S. Shimada sp. Nov.. Bull. Natl. Museum Nat. Sci. Ser. B, Bot. 40, 1–13.

Melton, J.T., Lopez-Bautista, J.M., 2020. Diversity of the green macroalgal genus *Ulva* (Ulvophyceae, Chlorophyta) from the east and gulf coast of the United States based on molecular data. J. Phycol. 57, 551-568

Platt, T., Gallegos, C.L., Harrison, W.G., 1980. Photoinhibition of photosynthesis in natural assemblages of marine phytoplancton J. Mar. Res. 38, 687-701.

Pringault, O., de Wit, R., Camoin, G., 2005. Irradiance regulation of photosynthesis and respiration in modern marine microbialites built by benthic cyanobacteria in a tropical lagoon (New Caledonia). Microb. Ecol. 49, 604-616.

Ralph, P.J., Gademann, R., 2005. Rapid light curves: A powerful tool to assess photosynthetic activity. Aquat. Bot. 82, 222-237.

Ralph, P.J., Gademann, R., Larkum, A.W.D., Kuhl, M., 2002. Spatial heterogeneity in active chlorophyll fluorescence and PSII activity of coral tissues. Mar. Biol. 141, 639-646.

Raven, J.A., Geider, R.J., 2003. Adaptation, acclimation and regulation in algal photosynthesis, in: Larkum, A.W.D., Douglas, S.E., Raven, J.A. (Eds.), Photosynthesis in Algae. Springer Netherlands, Dordrecht, pp. 385-412.

Richardson, K., Beardall, J., Raven, J.A., 1983. Adaptation of unicellular algae to irradiance - an analysis of strategies. New Phytologist 93, 157-191.

Scherner, F., Barufi, J.B., Horta, P.A., 2012. Photosynthetic response of two seaweed species along an urban pollution gradient: Evidence of selection of pollution-tolerant species. Mar. Pollut. Bull. 64, 2380-2390.

Schofield, O., Evens, T.J., Millie, D.F., 1998. Photosystem II quantum yields and Xanthophyll-cycle pigments of the macroalga *Sargassum natans* (Phaeophyceae): Responses under natural sunlight. J. Phycol. 34, 104-112.

Schreiber, U., Bilger, W., Neubauer, C., 1994. Chlorophyll fluorescence as a non-intrusive indicator for rapid assessment of in vivo photosynthesis, in: Schulze, E., Caldwell, M.M. (Eds.), Ecophysiology of Photosynthesis. Springer-Verlag, Berlin, pp. 49-70.

Thiers, B. 2019. Index herbariorum: a global directory of public herbaria and associated staff. New York Botanical Garden's Virtual Herbarium.

Torregiani, J.H., Lesser, M.P., 2007. The effects of short-term exposures to ultraviolet radiation in the Hawaiian Coral *Montipora verrucosa*. J. Exp. Mar. Biol. Ecol. 340, 194-203.

Uhrmacher, S., Hanelt, D., Nultsch, W., 1995. Zeaxanthin content and the degree of photoinhibition are linearly correlated in the brown alga *Dictyota-dichotoma*. Mar. Biol. 123, 159-165.

Wang, Y., Qu, T., Zhao, X., Tang, X., Xiao, H., Tang, X., 2016. A comparative study of the photosynthetic capacity in two green tide macroalgae using chlorophyll fluorescence. SpringerPlus 5, 775. https://doi.org/10.1186/s40064-016-2488-7

Whitehouse, L.N.A., Lapointe, B.E., 2015. Comparative ecophysiology of bloom-forming macroalgae in the Indian River Lagoon, Florida: *Ulva lactuca, Hypnea musciformis,* and *Gracilaria tikvahiae*. J. Exp. Mar. Biol. Ecol. 471, 208-216.

Williamson, C.J., Perkins, R., Yallop, M.L., Peteiro, C., Sanchez, N., Gunnarsson, K., Gamble, M., Brodie, J., 2018. Photoacclimation and photoregulation strategies of *Corallina* (Corallinales, Rhodophyta) across the NE Atlantic. Eur. J. Phycol. 53, 290-306.

Xie, W.F., Wu, C.H., Zhao, J., Lin, X.Y., Jiang, P., 2020. New records of *Ulva* spp. (Ulvophyceae, Chlorophyta) in China, with special reference to an unusual morphology of *U. meridionalis* forming green tides. Eur. J. Phycol. 55, 412–425.

Xu, Z., Wu, H., Zhan, D., Sun, F., Sun, J., Wang, G., 2014. Combined effects of light intensity and NH_4^+-enrichment on growth, pigmentation, and photosynthetic performance of *Ulva prolifera* (Chlorophyta). Chinese J. Oceanol. Limnol. 32, 1016-1023.

Zhang, X.W., Mou, S.L., Cao, S.N., Fan, X., Xu, D., Ye, N.H., 2015. Roles of the transthylakoid proton gradient and xanthophyll cycle in the non-photochemical quenching of the green alga *Ulva linza*. Estuar. Coast. Shelf Sci. 163, 69-74

Tables

Table 1. Fluorescence parameters, definition, implementation and derivation (adapted from Cosgrove and Borowitzka, 2010; Williamson et al., 2018)

Parameter	definition	Condition	Derivation
F'	The initial fluorescence intensity	Light incubated	
Fm'	The maximum intensity under saturating light	Light incubated	
Fm'm	The maximum value of Fm'	Light incubated	
Fq'	The fluorescence quenched in actinic light	Light incubated	$\mathrm{Fm'} - \mathrm{F'}$
Fq'/Fm'	Effective quantum efficiency of PSII	Light incubated	
F0	The minimum fluorescence yield (all RCIIs are open, dark-regulated)	Dark incubated	
Fm	The maximum fluorescence under saturating light (all RCIIs are open with NPQ negligible, dark-regulated)	Dark incubated	
Fv	The maximal variable fluorescence (dark-regulated)	Dark incubated	$\mathrm{Fm} - \mathrm{F0}$
Fv/Fm	Maximum quantum efficiency of PSII (dark-regulated)	Dark incubated	$\frac{\mathrm{Fm} - \mathrm{F0}}{\mathrm{Fm}}$
NPQ	Non photochemical quenching	Dark incubated	$\frac{\mathrm{Fm} - \mathrm{Fm'}}{\mathrm{Fm'}}$
PAR	Photosynthetically active radiation (µmol photons m^{-2} s^{-1})	Light & dark incubated	
rETR	Relative Electron transport rate (through PSII)	Light & dark incubated	$F_q'/F_m' \times PAR \times 0.5$
rETR(I)	Relative Electron transport rate (through PSII) as function of the irradiance and estimated by adjusting the model by Platt et al. (1980) to the rapid light curve data	Light & dark incubated	$rETR_m \times \left(1 - \mathrm{e}^{\left(-\alpha \times \frac{\mathrm{I}}{rETR_m}\right)}\right) \times \mathrm{e}^{\left(-\beta \times \frac{\mathrm{I}}{rETR_m}\right)}$
rETRmax	The maximum relative electron transport rate	Light & dark incubated	$rETR_m \times \left(\frac{\alpha}{\alpha+\beta}\right) \times \left(\frac{\beta}{\alpha+\beta}\right)^{\frac{\beta}{\alpha}}$
alpha (α)	The initial slope of the RLC at limiting irradiance	Light & dark incubated	
beta (β)	The slope when photoinhibition occurred	Light & dark incubated	
Ek	The light saturation index (µmol photons m−2 s−1)	Light & dark incubated	$\frac{rETR_{max}}{\alpha}$

Table 2. Results of the statistical analysis testing differences in photosynthetic parameters of *Ulva batuffolosa* between the five field campaigns. Photosynthetic parameters were obtained from rapid light curves performed light and dark incubated conditions. Statistical tests used were either ANOVAs or Kruskal-wallis tests (*). Fq'/Fm' and Fv/Fm stand for Effective and Maximum quantum light utilization efficiency of Photosystem II (PSII); $rETR_{max}$, maximum relative electron transport rate in AU; Ek, light saturation coefficient in μmol photons m^{-2} s^{-1}; alpha, maximum light utilization coefficient for PS II; beta, photoinhibition coefficient for PSII. Significant p-values (< 0.05) are bolded.

	Light incubated		Dark incubated	
	F-Ratio	P-Value	F-Ratio	P-Value
Fq'/Fm', Fv/Fm	2.60	0.100	3.70	**0.042**
$rETR_{max}$	8.32	**0.003**	13.32	**0.001**
Ek	15.48	**<0.001**	4.49	**0.025**
alpha	3.88	**0.037**	4.38	**0.027**
beta*		**0.034**		0.406

Table 3. Results of the general linear model analysis on Non-Photochemical Quenching (NPQ) of *Ulva batuffolosa* between the different field campaigns (month) and over the induction and dark recovery (light/dark condition). Significant p-values (< 0.05) are bolded.

	NPQ	
	F-Ratio	P-Value
A: Field campaign	86.20	**<0.001**
B: Light/dark condition	49.53	**<0.001**
A:B	1.83	**0.012**

Figure legends

Fig. 1. Study site. **A**. Location of the Poé-Gouaro-Deva (PGD) lagoon in New Caledonia. **B**. Satellite view of the PGD lagoon, highlighting the location of B21 station. The picture shows/points an underwater view of the green algal during a bloom of *Ulva batuffolosa* at this station.

Fig. 2. Environmental conditions that characterized the PGD area over the study period. **A.** Temperature, at B21 station, as recorded by loggers (solid line) or satellite derived SST (grey dashed line). Grey ribbon delimits the daily minimum and maximum temperature recorded by *in situ* loggers. **B**. Surface Solar Radiation Downwards (SSRD). Note that night values were not discarded to compute this time series, but were discarded to compute values reported in the main text. Dashed red lines mark the five sampling campaigns, respectively on the 16th May 2019, 09th July 2019, 18th November 2019, 19th February 2020, and 25th May 2020.

Fig 3. Algal biomass (g Dry Weight m^{-2}) recorded during field campaigns along transects with corresponding under water images for illustration. Letters indicate significant differences between campaigns (p-value < 0.05). Data are expressed as mean ± standard deviation (SD, n = 3).

Fig. 4. A. Effective (Fq'/Fm') and **B.** Maximum quantum light utilization efficiency of the photosystem II (PSII, Fv/Fm) measured under ligh and dark incubated conditions, respectively, for *Ulva batuffolosa* collected in the PGD lagoon during the five field campaigns. Data are expressed as mean ± standard error (SE, n = 3) and * indicates significant differences between field campaigns (p-value < 0.05).

Fig. 5. A. Light and **B.** Dark incubated rapid light curves (RLC, n=3) expressed as the relative electron transport rate (rETR) as a function of the photosynthetic active radiation (PAR in µmol photons m^{-2} s^{-1}) of *Ulva batuffolosa* in PGD lagoon over one year. Data are expressed as mean ± standard deviation (SD, n = 3).

Fig. 6. Photosynthetic parameters obtained from rapid light curves carried out on light (yellow) and dark (grey) incubated *Ulva batuffolosa* during the different field campaigns. **A.** Maximum electron transport rate, $rETR_{max}$ in AU, **B.** light saturation coefficient, Ek in µmol photons m^{-2} s^{-1}, **C.** Maximum light utilization coefficient for photosystem II, alpha, **D.** photoinhibition coefficient for photosystem II, beta. Data are expressed as mean ± standard error (SE, n = 3) and different letters indicate statistically significant differences ($p < 0.05$).

Fig. 7. Non-Photochemical Quenching (NPQ) over the induction (yellow background) and dark recovery (grey background) of *Ulva batuffolosa* sampled at the different period of the year and dark incubated. Data are expressed as mean ± standard deviation (SD, n = 3) and different letters (cf. caption) indicate statistically significant differences between field campaigns ($p < 0.05$).

Figures

Fig. 1

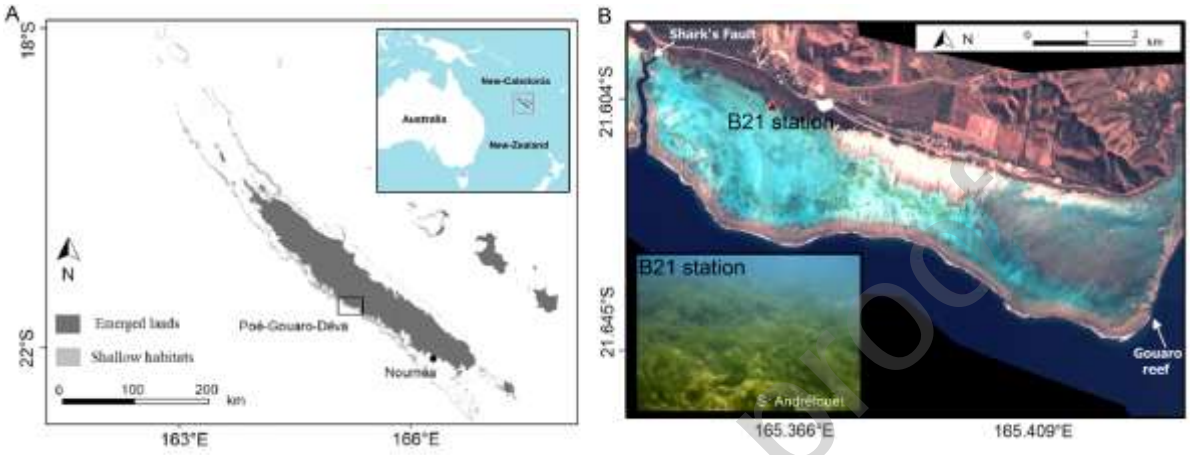

Fig. 2

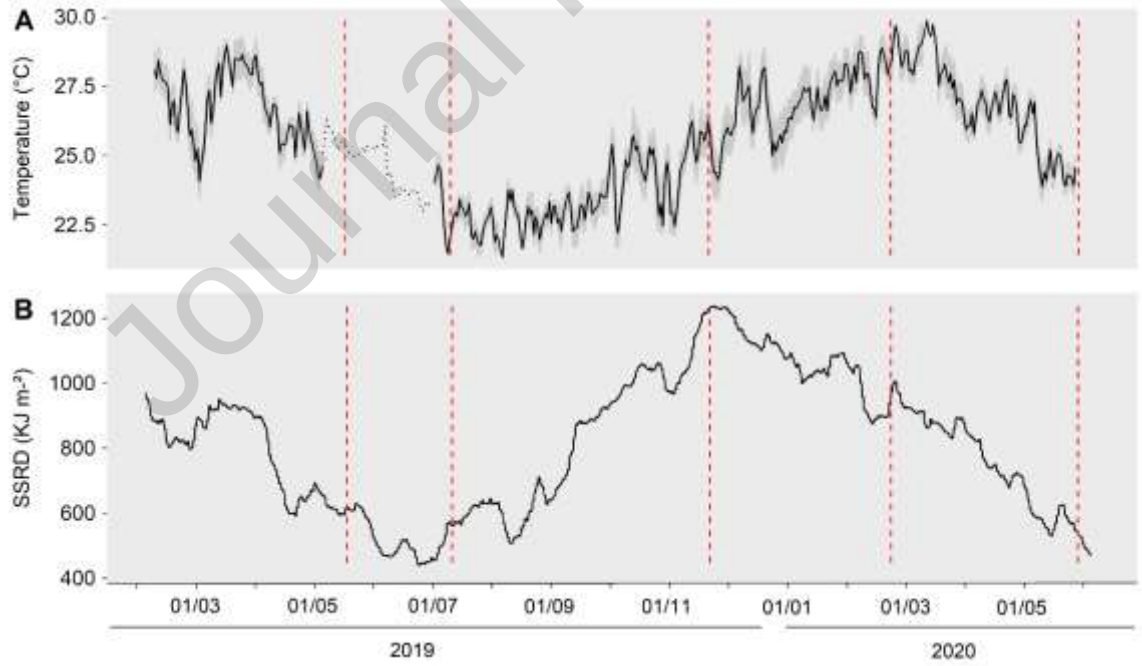

Fig. 3

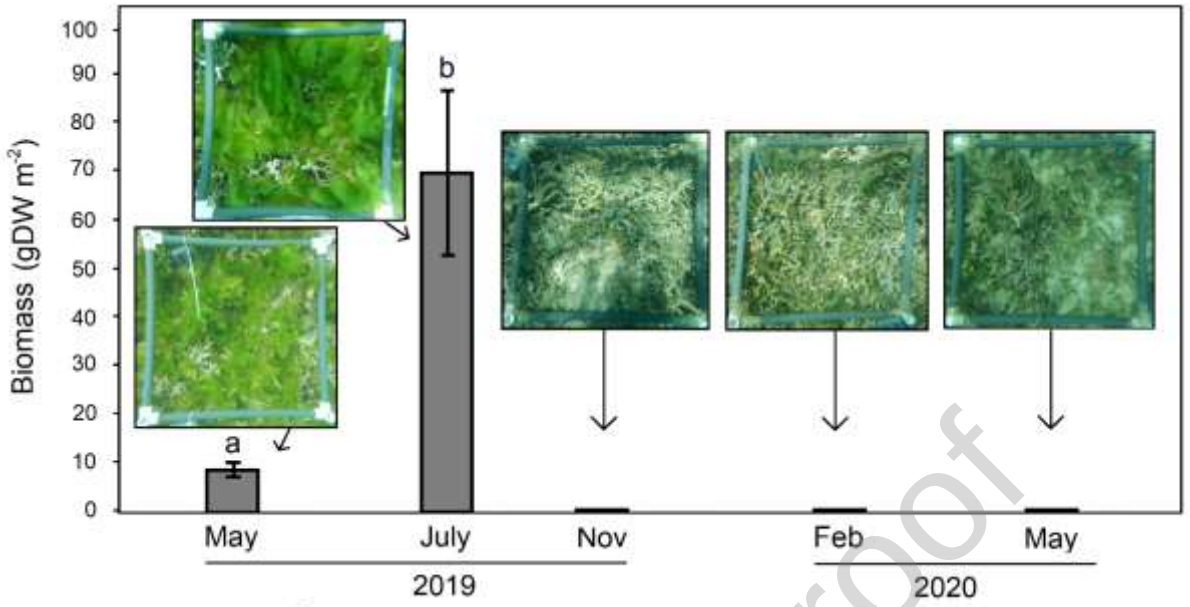

Fig. 4

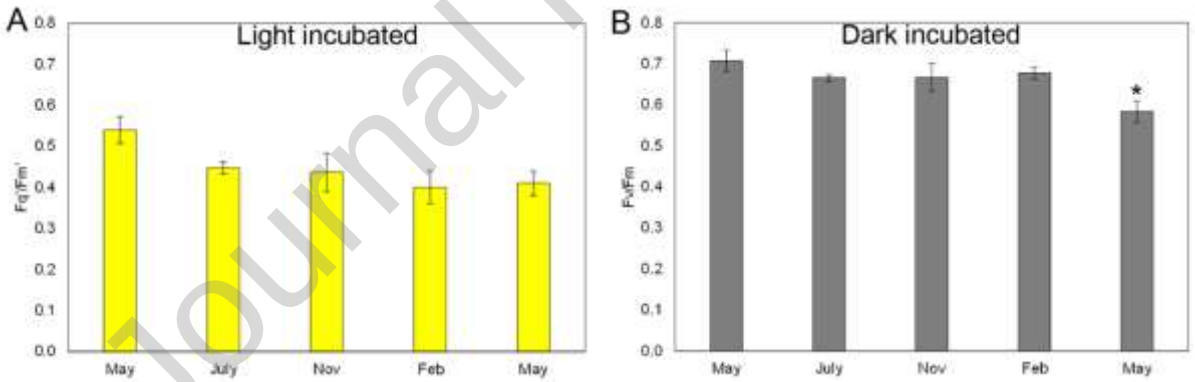

Fig. 5

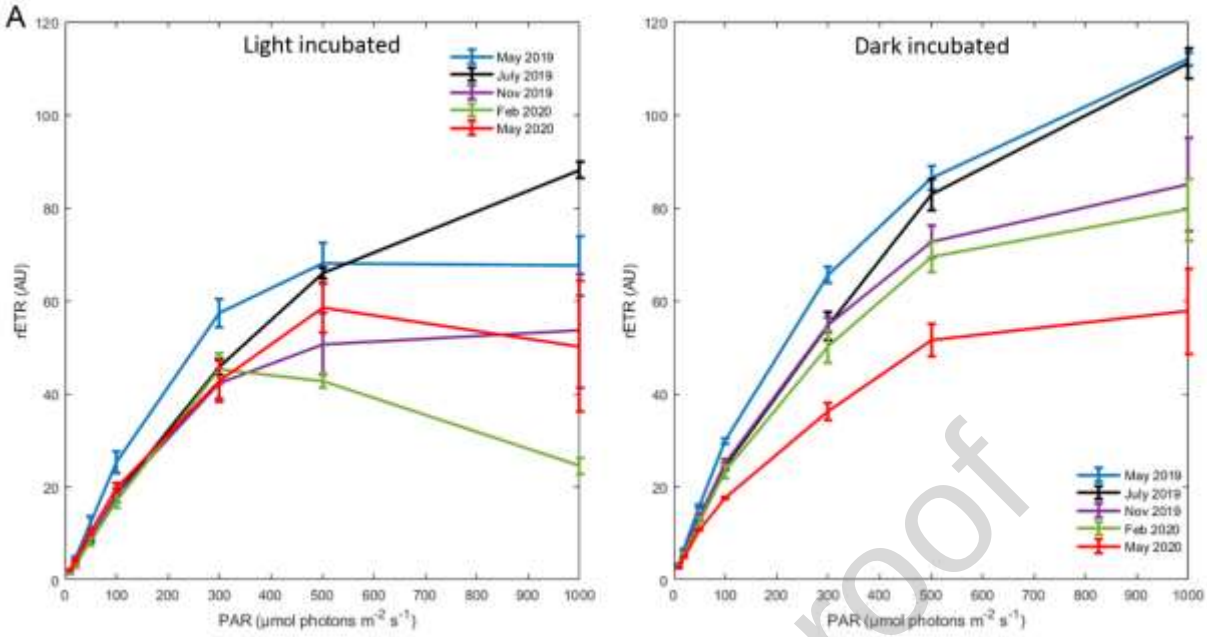

Fig. 6

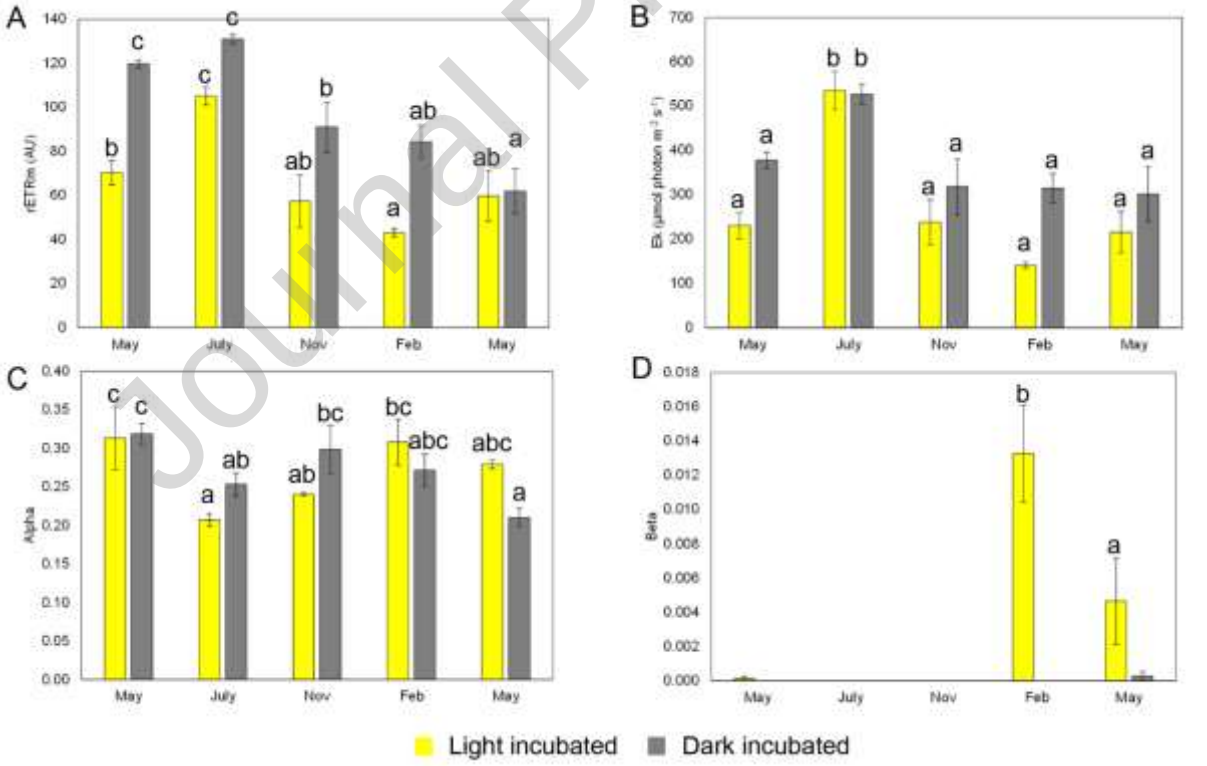

Fig. 7

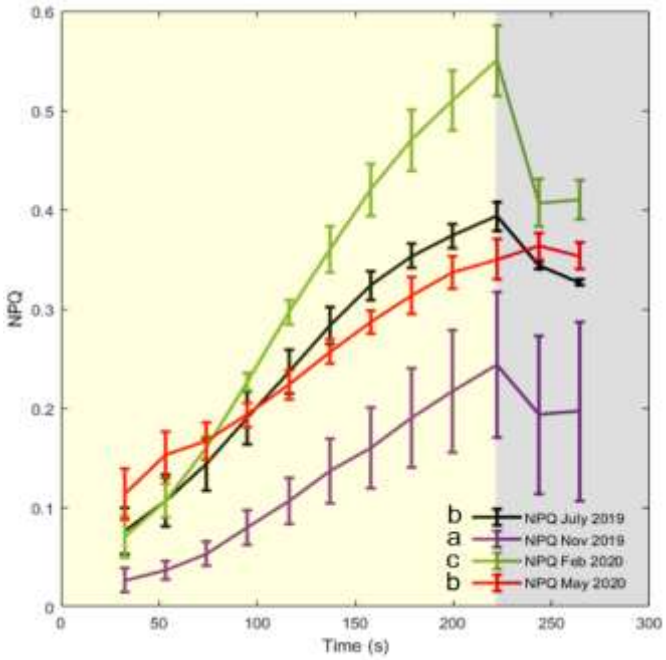

Author statement

On behalf of all the co-authors, we declare that all authors have seen and approved the final version submitted, all of the reported work is original, and that all prevailing local, national international regulations and conventions, and normal scientific ethical practices, have been respected.

In addition, this manuscript or a very similar manuscript has not been published, nor is under consideration by any other journal.

Declaration of interests

☒ The authors declare that they have no known competing financial interests or personal relationships that could have appeared to influence the work reported in this paper.

☐The authors declare the following financial interests/personal relationships which may be considered as potential competing interests:

Highlights :

- Photo-acclimation and regulation status of *Ulva batuffolosa* were modulated by season
- *Ulva batuffolosa* was well adapted to support and tolerate high irradiance
- The combination of elevated temperatures and light damaged its physiology